Silicon Spring Blades At Cryogenic Temperatures

Kiernan Reising
Georgia College & State University and
kiernanreising@gmail.com

Prof. Giles Hammond and Dr. Alan Cumming
Institute of Gravitational Research and
University of Glasgow

University of Florida's International REU Gravitational Physics Program

Third-generation gravitational wave detectors will be underground and lowering to cryogenic temperatures. Part of building third-generation detectors is lowering the noise of the suspension system. Particularly, the spring blades from which the silica fibers hold up the test mass and mirrors. In this research project, a theoretical model of all the modes using ANSYS was built and compared with measured modes, then using the measured modes to look into the effects of the young modules from 77 to 300 kelvin. While also using the data collected from the cryostat looking into ring down times and mechanical loss of the spring blades. The main goal of this research is to start building towards the silicon spring blades that will be in third-generation gravitational wave detectors.

I. INTRODUCTION

A major role in detecting gravitational waves is the upgrades that go into the detectors. The main purpose of these upgrades is to increase the sensitivity, by lower noise sources. Some of the noise sources that exist in gravitational wave detectors are thermoelastic noise, quantum noise, and seismic noise. This project work with the thermoelastic noise source, which comes from the internal dissipation of the spring blades. In this project, we investigate the use of silicon spring blades at cryogenic temperatures, so that we can lower the mechanical loss of the silicon spring blades, which should be dominated by the thermoelastic loss at higher temperatures.

II. THEORETICAL MODEL

Mathematical Model: Part of the building a theoretical model is starting with a simple mathematical model. The mathematical model used in this project is derived from a triangular cantilever beam with a fixed end and a free end with an applied load.

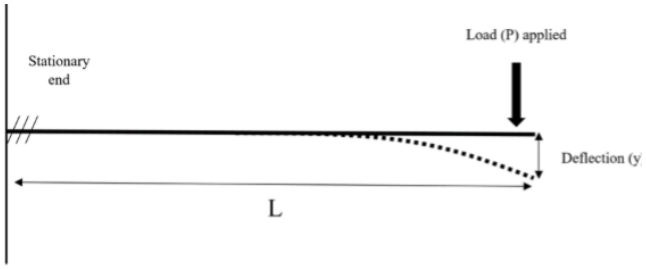

The bending moment (M_x) is given by the equation below [] .

$$M_x = P(L - X) \quad (3.1)$$

The P in the equation is the load applied to the cantilever, L and X are the length of the cantilever and the position along the cantilever respectively.

$$\frac{d^2y}{dx^2} = \frac{M_x}{EI} \quad (3.2)$$

Here the E and I are the young's modulus and moment of inertia respectively, and the equation above gives us the moment of curvature. Based on the triangle cantilever in figure1, the area moment of inertia is given by:

$$I = \frac{wt^3}{12}\frac{(L-X)}{L} \quad (3.3)$$

The width and thickness are written as w and t. By combining equations 3.2 and 3.3, the equation for the moment of curvature becomes:

$$\frac{d^2y}{dx^2} = \frac{M_x}{E}\frac{12}{wt^3}\frac{L}{(L-X)} \quad (3.4)$$

Plugging in equation 1.1 into the equation above gives:

$$\frac{d^2y}{dx^2} = \frac{P(L-X)}{E}\frac{12}{wt^3}\frac{L}{(L-X)} (3.5)$$

$$\frac{d^2y}{dx^2} = \frac{12PL}{Ewt^3} \quad (3.6)$$

Next by multiplying the dx^2 to both sides and then integrating the equation results in the equation below:

$$dy = (\frac{12PLx}{Ewt^3} + a)dx \quad (3.7)$$

By setting x in equation blank to zero gives us the constant $a = 0$. This allows us to integrate again, and produce the equation for the deflection of the cantilever beam(which is denoted by the symbol y).

$$y = \frac{12PLx^2}{Ewt^3} + b \quad (3.8)$$

The b in the equation above is again equal to zero by following the same process as before. Then equation blank just becomes:

$$y = \frac{12PLx^2}{Ewt^3} \quad (3.9)$$

This leads us to the next part of our mathematical model the natural frequency. We derived this model by giving the spring an intrinsic stiffness. The stiffened is given by the variable k, which is the mathematical representation the range of the cantilever beam deflection.

$$k = \frac{P}{y} = \frac{Ewt^3}{6L^3} \quad (3.10)$$

From here we can now calculate the natural frequencies using the equation below:

$$f = \frac{1}{2\pi}\sqrt{\frac{k}{m}} \quad (3.11)$$

Finite Element Analysis: The second part in developing our theoretical model is to model the actual spring blades using Solid Works, and then transferring the Solid Works file to ANSYS for finite element analysis.

Dimensions of Single Silicon Spring Blades		
Blade Type	Length (mm)	Width (mm)
C1	85.00	42.50
C2	80.00	35.00
HS1	90.00	22.50
HS2	90.00	20.00
HS3	80.00	15.00
DB1M	30.93	20.00
DB1A	23.43	10.00
DB1AM	54.36	20.00
DB2M	27.9	30.00
DB2A	20.4	15.00
DB2AM	48.3	30.00
KOA	54.6	21.00
KOM	48.4	31.7
AEI	60.00	15.00

Using the dimensions from the table above an ANSYS model for purely triangular blades was constructed, and then the triangular ANSYS model was compared to the mathematical model for triangular blades. The meshing for the FEA model was refined to one millimeter, to account for any overlooked elements in the spring blades.

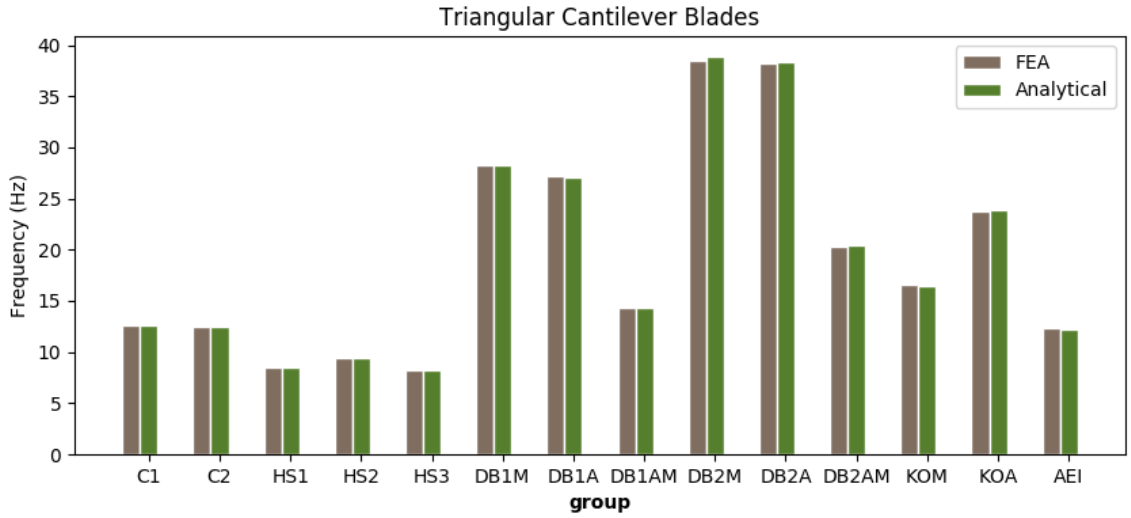

FIG. 1: This shows the comparison of the mathematical and ANSYS model for triangular cantilever blades and allows us to investigate the use of ANSYS as a possible source for building a theoretical model for silicon spring blades

The bar graph above demonstrates that the ANSYS model and mathematical model come quite close to each other, with minor differences in the shorter blades. We can now model the actual blades that are available for measurements. We also meshed these blades to one millimeter. Next, we compared the blade again to the mathematical model

The figure above shows the differences between the mathematical model and the ANSYS model. Differences in the frequencies suggest that the clamping endings have an effect on the frequencies that are predicted by the ANSYS model. This model only accounts for the single blades, and now we need to add in the double and triple blades. Below are the dimensions for the double and triple spring blades.We used an existing Solidworks file containing all the double and triple spring blades, and was used for F.E.A modeling in ANSYS, this step was taken because it would speed up the processes of constructing a theoretical model, and the SolidWorks wafer contains the blades the are ready to be measured.

Above is the ANSYS model for silicon spring blades, which predict up to the first six modes of each spring blade.

of Cantilever Blades.png

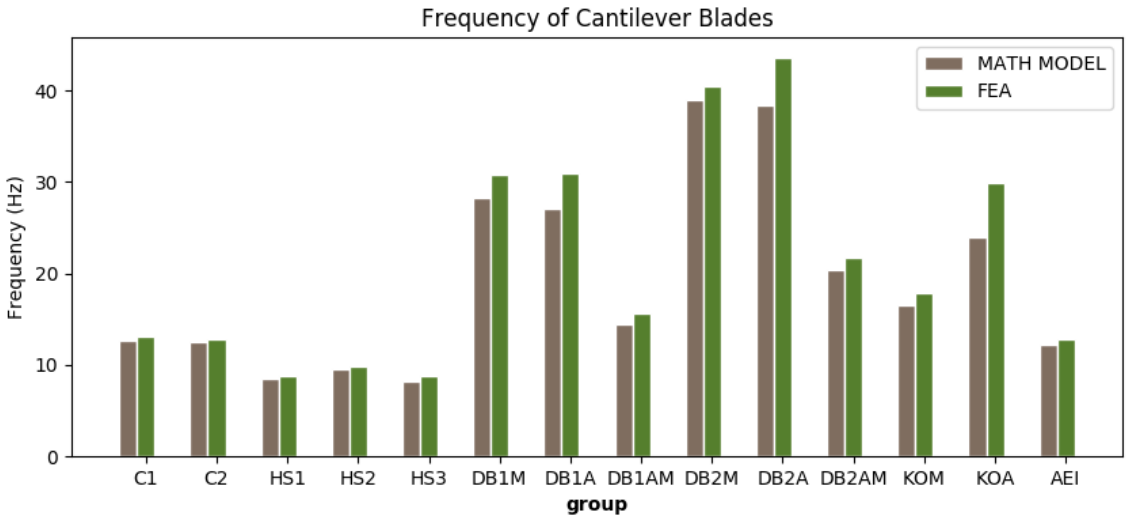

FIG. 2: Similar to figure before this figure compares the mathematical model and ANSYS model, however the ANSYS model now use the clamping ends of the blades.

Dimensions of Double and Triple Blades		
Blade Type	Length (mm)	Width (mm)
DB1	40.00	75.00
DB2	40.00	80.00
DBS1	40.00	75.00
DBS2	40.00	80.00
KO	90.00	46.00
TB1	100.0	100.00
TB2	50.00	100.00

FIG. 3: This figure gives us the dimensions for the double and triple spring blades.

The model is only for single spring blades with a point mass attached to it, to get the frequencies of the spring blades without the point mass we have built another model. The model for single silicon spring blades without a point mass can be view by the chart below.

ANSYS Modes For Single Silicon Spring Blades Without a Point Mass						
Blade Type	1rst Mode	2nd Mode	3rd Mode	4th Mode	5th Mode	6th Mode
C1	230.83	959.44	1761.6	2298.6	4276.5	4321.4
C2	263.34	1121.6	2219.8	2665.3	4896.4	5405.6
HS1	200.68	848.53	2057	2756.9	3846.7	4292.6
HS2	246.7	1042.9	2540.2	3419	4703.9	4773.8
HS3	228.65	1004.6	2503.2	3400.4	4150.4	4745.1
DB1M	1130.1	4401.3	6971.7	10464	18384	19858
DB1A	1399.2	6026.2	13108	15117	15462	29961
DB1AM	433.69	1823.3	4241.8	4417.7	8286.4	8743.9
DB2M	1453.1	5281	5926.4	11596	16565	16945
DB2A	1848.3	7744.7	10520	18865	27806	29018
DB2AM	585.08		3595.7	5440	9176.2	9993.9
KOA	447.42	2001.7	4333.2	5043.1	9215.3	9607.8
KOM	411.87	1698.8	2583.4	4117.8	6432.9	7743.7
AEI	409.28	1691.91	4202.9	5662.9	5966.1	8049.1

The next two charts show the ANSYS models for double and triple blades with and without point masses

ANSYS Modes For Single Silicon Spring Blades With a Point Mass						
Blade Type	1rst Mode	2nd Mode	3rd Mode	4th Mode	5th Mode	6th Mode
C1	13.03	314.9	558.7	558.7	1770.4	2074.7
C2	12.865	237.68	614.72	614.72	2195.5	2226.6
HS1	8.8372	128.31	496.92	496.48	1785.4	2760.4
HS2	9.8899	131.43	607.39	607.39	2180.5	3423.5
HS3	8.7154	100.07	601.17	601.17	2164	4146.4
DB1M	30.747	346.32	1463.5	1463.5	7001.8	8967.5
DB1A	30.968	267.87	1458.5	1458.5	13129	13435
DB1AM	15.581	214.72	950.5	950.43	3692.3	4253
DB2M	40.396	429.39	1541.1	1541.1	5952	10023
DB2A	40.642	480.16	1685.1	1685.1	10607	16201
DB2AM	21.648	321.74	1105.5	1105.1	3610	4449
KOA	17.897	298.88	1130.8	1130.8	4326.3	4356.7
KOM	29.938	568.07	1016.3	1016.3	2608	3645.5
AEI	12.803	128.41	903.34	903.34	3663.2	5965.1

FIG. 4: In this figure, we have the first six modes, with a point mass attached at the end of the spring blade give the blade its applied load.

ANSYS First Mode For Double and Triple Silicon Spring Blades Without a Point Mass	
Blade Type	1rst Mode
DB1	353.89
DB2	387.62
DBS1	344.58
DBS2	247.34
KO	104.79
T1	41.671
T2	180.44

FIG. 5:

respectively.

Due time restrictions, only the first mode was predicted for the double and triple blades, however, they still serve as a good starting point for future work. Some interesting things to look into would be is the difference between the T1 and T2 modes. Based on the comparison of the mathematical model and ANSYS model, we can see that the F.E.A in ANSYS model does hold a good approximation for predicting the spring blade's modes. One of the strongest features of the ANSYS model is not only allowed to account for the ends of the blade but also have predictions for double and triple blades that the mathematical model does not provide. Since the mathematical model is only limited to purely triangular cantilever beams, we choose to use the ANSYS model we bit as the predictions for the modes in the cryostat.

III. EXPERIMENTAL SET UP

This section will go over how the experiment was conducted and set up. Before we go on, it is important to note, that in this experiment we, are only using spring blades with no applied load. The objectives of this experiment were to investigate the mechanical loss and young's modulus as a function of temperature.

Set Up:

ANSYS First Mode For Double and Triple Silicon Spring Blades With a Point Mass	
Blade Type	First Mode
DB1	22.199
DB2	26.937
DBS1	28.528
DBS2	36.327
KO	8.5784
T1	5.707
T2	16.917

FIG. 6:

Before the cryostat was open, the lasers and vacuum pumps were disconnected. The two silicon blades were picked blindly and put in the cryostat, and the clamped down by using the allen key. Then cryostat was closed and gently flipped it back right side up. Then the lasers and vacuum pumps were reconnected. After we reconnected the lasers and vacuum pumps, we waited till the vacuum pumps dropped the pressure to $1.5 * 10^{-7} mbar$. Dropping the pressure in the cryostat to $1.5 * 10^{-7} mbar$ allows us to fill the cryostat with liquid nitrogen without it boiling off. Electrostatic drives above the spring blades are given a voltage to excite their modes. Modes of the spring blades can be measured by using mirrors at an angle inside of the cryostat. The lasers then reflect off the mirrors inside the cryostat on to the spring blades, from there laser exits the cryostat into the photodiode allowing us to measure the frequencies. Then the interval from $77 - 300$ Kelvin for measurements can be obtained by increasing the temperature on the heater to above the temperature of the clamps and cryostat.

Methodology:
Before pumping liquid nitrogen into the cryostat, we did a long-range scan at room temperature for the first six modes of each sample. We found at room temperature that the blades resembled the frequencies of HS2 in channel one and HS1 in channel 2. We then started to pump the cryostat full of liquid nitrogen. Once the cryostat was down to 77 Kelvin we started to take measurements. Using the ANSYS modeled frequencies of blades HS1 and HS2 as a tool to help find the frequencies at 77 Kelvin. We expected the frequencies to increase because the stiffness would increase at cryogenic temperatures, so we made an interval for the modes longer in the higher frequency range. After we were able to find the modes using the LabView program at 77 Kelvin, we then found the ringdown times at 77 Kelvin. The only modes found were the first four for channel one and the first two for channel two. After that, we started to increase the temperature in intervals of five. From this point, the cryostat was left overnight to take measurements.In the morning it was found that the cryostat had only reached measurement to 220 Kelvin, unfortunately, reliable measurements after this point were hard because the temperature was already over 220 in the cryostat, because of this it was decided to cool down the cryostat again and do another run form $77 - 300$ Kelvin. The second run, we decided to do 20 Kelvin intervals instead of 5, with a gap between 200 and 220 to speed up the processes. After we collected all the data from the cryostat run, we moved on to data analysis.

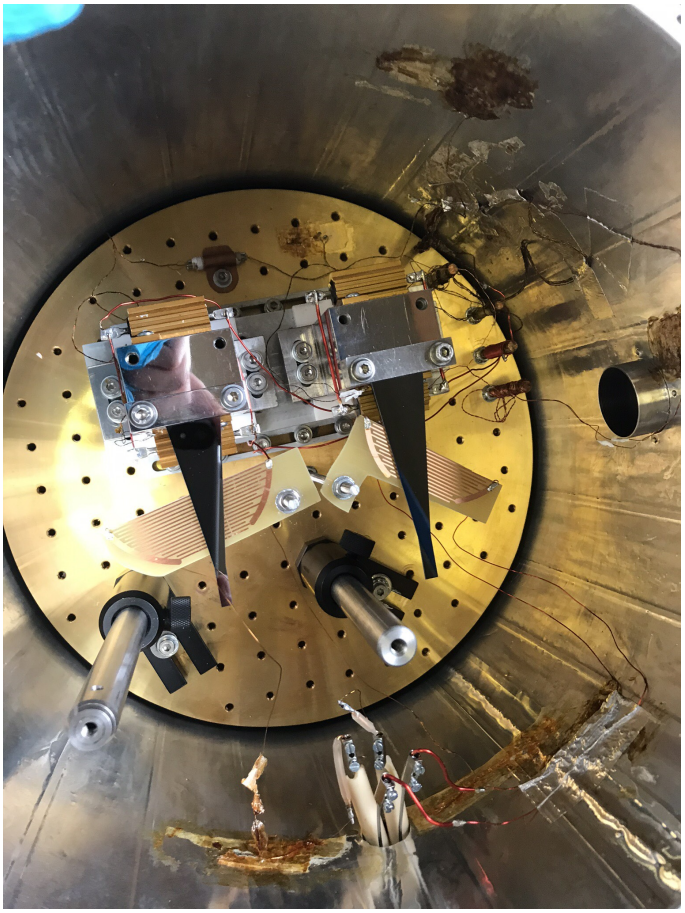

FIG. 7: This figure shows the inside of the cryostat. Note that the cryostat is upside down. On the left is the channel one sample, and to the right is the channel two sample

FIG. 8: Here the cyrostat is being pumped full of liquid nitrogen

IV. RESULTS AND ANALYSIS

This section looks into the results of the experiment, particularly the mechanical loss and frequencies from 77 to 300 Kelvin. We also looked into the change of the young's modulus as a function of temperature. These efforts are all for a better understand silicon at cryogenic temperatures.

Channel One Silicon Spring Blades Sample:

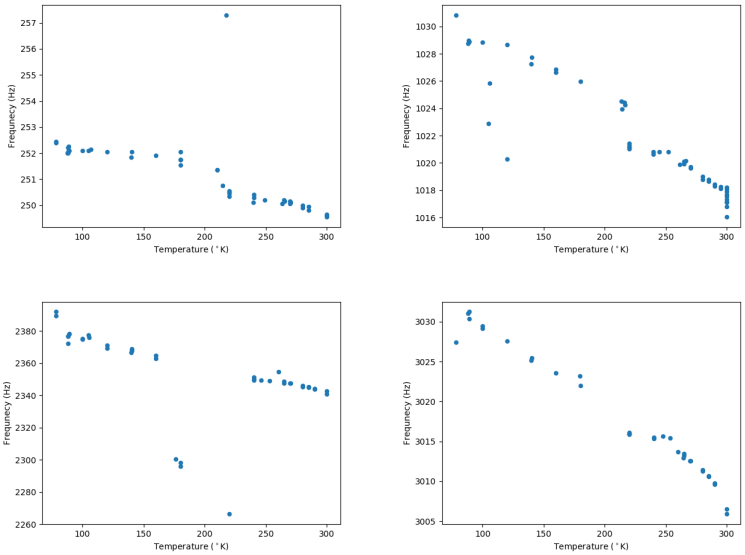

FIG. 9: This figure shows the change in frequencies vs. temperature for the sample in channel one.The first two modes are on the top row, with increasing order to the right. The third and fourth are on the bottom row, also with increasing order to the right.

Channel Two Silicon Spring Blades Sample:

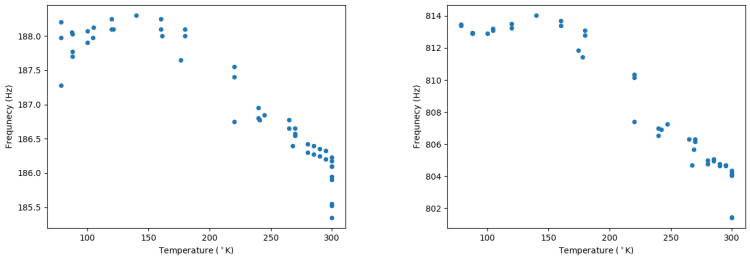

1.*png*

FIG. 10: This figure shows the change in frequencies vs. temperature for the sample in channel two.The first mode is on the left and the second is on the right

The change in frequencies vs. temperature for both samples show the frequencies decreasing as temperature increase for 77 to 300 Kelvin. This relationship tells us that the silicon spring blade becomes stiffer at lower temperatures, which was an expected result.

We were able to find the mechanical loss for silicon blades by using a pre-written Matlab script. The Matlab script follows the process below.

First, we find the ringdown time, which follows has an exponential decay:

$$y = y_0 e^{-\gamma t} (5.1)$$

Then we take the natural log of equation 5.1:

$$ln(y) = Y_0 - \gamma t (5.2)$$

From equation 5.2 we can find γ by plotting $ln(y)$ vs. t, and then plug γ into the Q equation below:

$$Q = \frac{w_0}{\gamma} (5.3)$$

Next we take the inverse of Q, giving us the mechanical loss:

$$\phi = \frac{1}{Q} (5.4)$$

Mechanical Loss Measurement For Channel One:

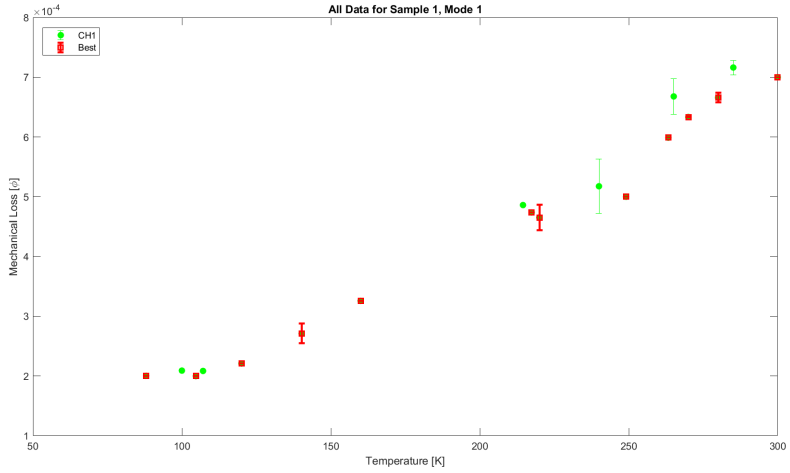

FIG. 11: This figure shows the change in mechanical loss vs. temperature for the first mode

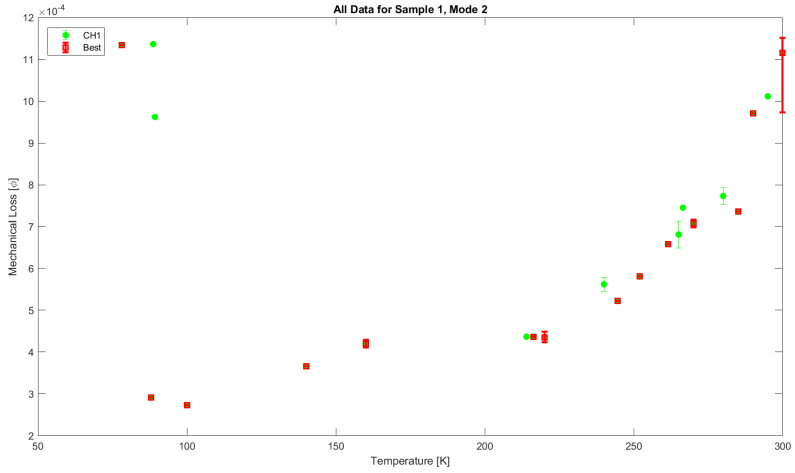

FIG. 12: This figure shows the change in mechanical loss vs. temperature for the second mode

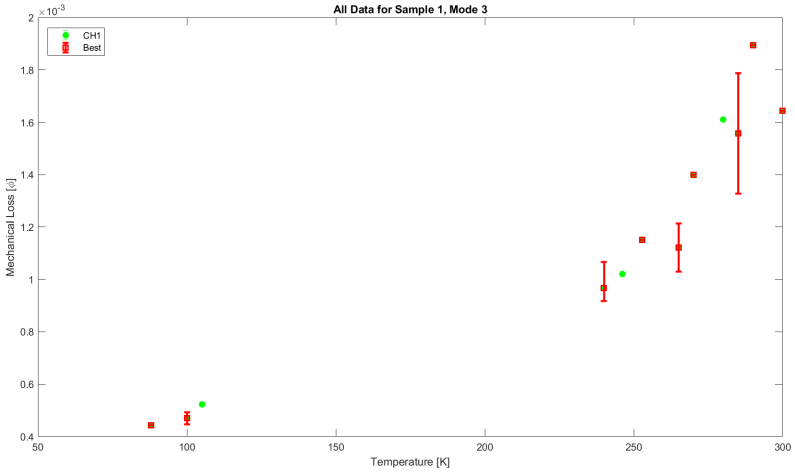

FIG. 13: This figure shows the change in mechanical loss vs. temperature for the third mode

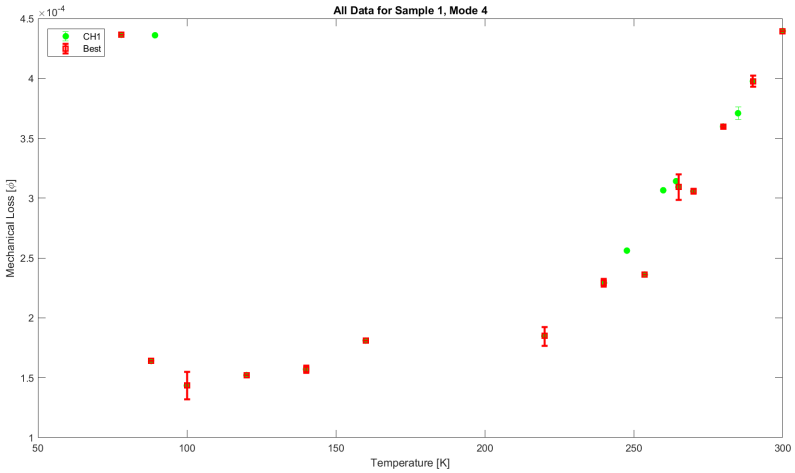

FIG. 14: This figure shows the change in mechanical loss vs. temperature for the fourth mode

Mechanical Loss Measurements For Channel Two:

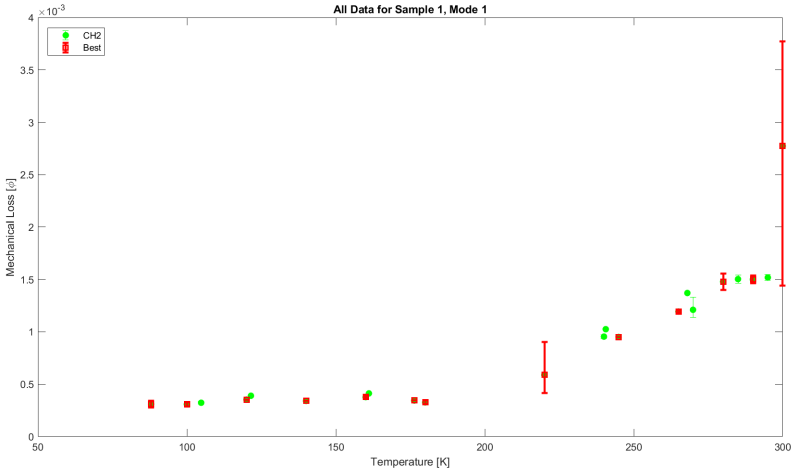

FIG. 15: This figure shows the change in mechanical loss vs. temperature for the first mode

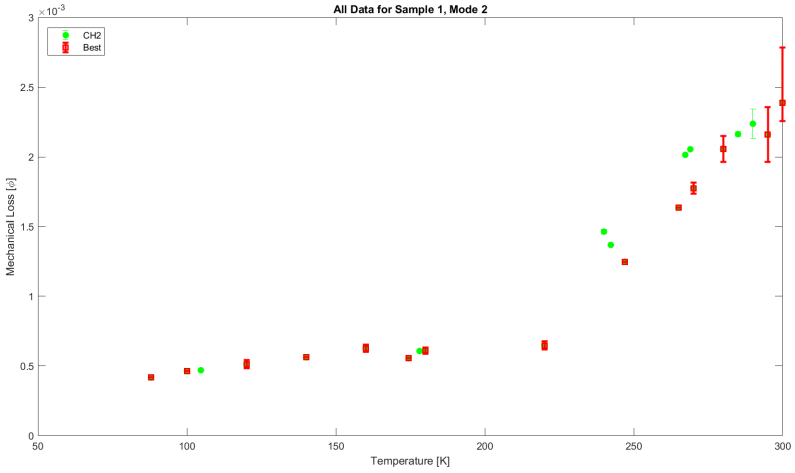

FIG. 16: This figure shows the change in mechanical loss vs. temperature for the second mode

After we had pulled the spring blade samples out the cryostat, we found out that the blades had belonged to an earlier wafer. What this meant is that we had to go back into ANSYS and remodel the blades based on what blades were actual in the cryostat. Below is the new ANSYS model of the two blades that were in the cryostat.

ANSYS Modes For Single Silicon Spring Blades Without a Point Mass						
Blade Type	1rst Mode	2nd Mode	3rd Mode	4th Mode	5th Mode	6th Mode
Channel One Sample	208.12	860.46	2142.3	2737.6	4108.7	5563.3
Channel Two Sample	151.94	655.28	1655.7	2123.8	3184.3	4450.8

Now, based on the new model, it is easy to see that, the ANSYS frequencies don't quite line up with the measured frequencies. We wanted to see if the change in the young's modulus while changing the temperature is what is causing these differences. The way we went about this was by using calculating the residual frequency for a single temperature. The residual frequency is the sum of the squared difference between the measured frequencies and theoretical frequency.

Residual formula:

$$R = (M_1 - T_1)^2 + (M_2 - T_2)^2 + (M_3 - T_3)^2 + ...$$

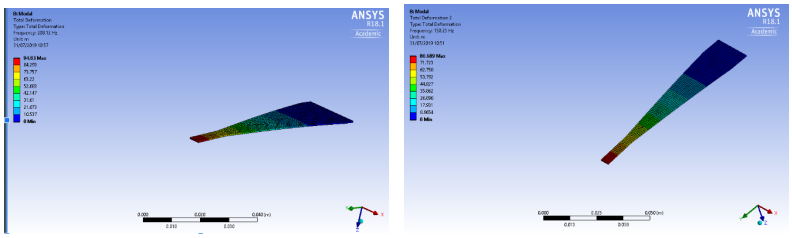

FIG. 17: On the left is the blade that was in channel one, and on the right the blade that was in channel two

Using the frequencies from ANSYS and the cryostat, we wrote a python code that would plot the residual vs. the young's modulus. The python code would then find the global minimum, and at whatever young modulus you are at that would become the young's modulus for the given temperature.

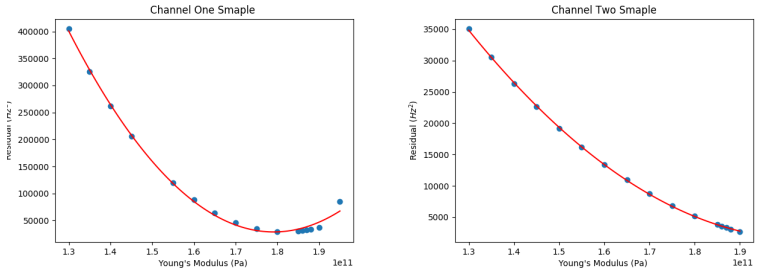

FIG. 18: This figure shows the plot of the residual vs. young's modulus for both blades

Based on the figure above we can see that channel one sample has global minimum, where as channel two sample does not. We still have not found a reason as to why channel two does not have a global minimum. Using the data from channel we were able to find the young's modulus a function of temperature.

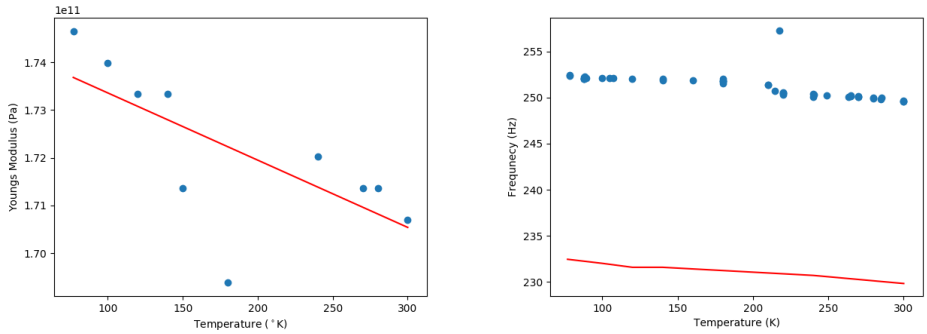

FIG. 19: The first image is the young's modulus vs. temperature. The second image is the frequency vs. temperature, with the ANSYS model adjusted for the young's modulus change with temperature. The ANSYS model is the first mode of the sample in channel one

When we compared our new ANSYS model to the cryostat measurements, finding that even when adjusting for the young's modulus change with temperature, the ANSYS model still did not line up with the measured frequencies. First, this tells us that the young's modulus is not the only factor that contributes to the difference between the ANSYS and the measured frequency. This also suggests that the ANSYS model may have some unknown

factor because the ANSYS frequencies were expected to be higher than the measured frequencies since ANSYS models the blades as infinitely stiff.

V. CONCLUSION

The main goal of this experiment was to investigate the change in frequency and mechanical loss as a function of temperature. We found that the measured frequencies decreased as the temperature increased from $77 - 300$ Kelvin. This relationship showed that the spring blades stiffness increases at lower temperatures. Our mechanical loss measurements showed that the thermoelastic loss was dominant at higher temperatures. The ANSYS model did line up with the mathematical model of the triangular cantilever, which means that ANSYS is still a good theoretical model, but more investigating into ANSYS needs to be done in order create a more precise theoretical model.

VI. FUTURE WORK

This study was a step in the right direction, for investigating silicon spring blades at cryogenic temperatures. Future work should look into many different subjects of silicon spring blades at cryogenic temperatures. The ANSYS model would be something to continue to look at, in that ANSYS much lower frequencies than expected. More work also could by doing F.E.A of the clamping system inside the cryostat. Looking into other factors that may also contribute to the differences in frequencies would also be interesting.

VII. ACKNOWLEDGMENTS

I would like to thank the University of Florida for setting up this program, and the National Science Foundation for funding it. Also, thank you to the University of Glasgow for being the best host. I am very grateful took have worked with Prof. Giles Hammond and Dr. Alan Cumming as my advisors. Thank you to Peter, Simon, and Ian for helping me out in the lab, and answering any questions I had. Also thank you, to the Ph.D. students like Mark, Joe, and Andrew for making me feel welcome.

VIII. REFERENCES

[1] A V Cumming et al 2012 Class. Quantum Grav. 29 035003

[2] G D Hammond et al 2012 Class. Quantum Grav. 29 124009

[3] K Toland et al 2018 Class. Quantum Grav. 35 165004

[4] Toland, Karl William (2015) Development and characterisation of a pulling machine to produce small diameter silica fibres for use in prototype advanced gravitational wave detectors. MSc(R) thesis, University of Glasgow.

[5] Gere, J., Mechanics of Materials. 2004.